mAbs

ISSN: 1942-0862 (Print) 1942-0870 (Online) Journal homepage: http://www.tandfonline.com/loi/kmab20

Knobs-into-holes antibody production in mammalian cell lines reveals that asymmetric afucosylation is sufficient for full antibody-dependent cellular cytotoxicity

Whitney Shatz, Shan Chung, Bing Li, Brett Marshall, Max Tejada, Wilson Phung, Wendy Sandoval, Robert F Kelley & Justin M Scheer

To cite this article: Whitney Shatz, Shan Chung, Bing Li, Brett Marshall, Max Tejada, Wilson Phung, Wendy Sandoval, Robert F Kelley & Justin M Scheer (2013) Knobs-into-holes antibody production in mammalian cell lines reveals that asymmetric afucosylation is sufficient for full antibody-dependent cellular cytotoxicity, mAbs, 5:6, 872-881, DOI: 10.4161/mabs.26307

To link to this article: http://dx.doi.org/10.4161/mabs.26307

mAbs 5:6, 872–881; November/December 2013; © 2013 Landes Bioscience

Knobs-into-holes antibody production in mammalian cell lines reveals that asymmetric afucosylation is sufficient for full antibody-dependent cellular cytotoxicity

Whitney Shatz[1], Shan Chung[2], Bing Li[3], Brett Marshall[4], Max Tejada[4], Wilson Phung[1], Wendy Sandoval[1], Robert F Kelley[3], and Justin M Scheer[1,*]

[1]Department of Protein Chemistry; Genentech, Inc; San Francisco, CA USA; [2]Department of BioAnalytical Sciences; Genentech, Inc; San Francisco, CA USA; [3]Department of Antibody Engineering; Genentech, Inc; San Francisco, CA USA; [4]Department of Biological Technologies; Genentech, Inc; San Francisco, CA USA

Keywords: knobs-into-holes, glycosylation, effector function, afucosylation, ADCC, asymmetric antibody, symmetry, heterodimer

Knobs-into-holes is a well-validated heterodimerization technology for the third constant domain of an antibody. This technology has been used to produce a monovalent IgG for clinical development (onartuzumab) and multiple bispecific antibodies.[1,2] The most advanced uses of this approach, however, have been limited to *E. coli* as an expression host to produce non-glycosylated antibodies. Here, we applied the technology to mammalian host expression systems to produce glycosylated, effector-function competent heterodimeric antibodies. In our mammalian host system, each arm is secreted as a heavy chain-light chain (H-L) fragment with either the knob or hole mutations to allow for preferential heterodimer formation in vitro with low levels of homodimer contaminants. Like full antibodies, the secreted H-L fragments undergo Fc glycosylation in the endoplasmic reticulum. Using a monospecific anti-CD20 antibody, we show that full antibody-dependent cell-mediated cytotoxicity (ADCC) activity can be retained in the context of a knobs-into-holes heterodimer. Because the knobs-into-holes mutations convert the Fc into an asymmetric heterodimer, this technology was further used to systematically explore asymmetric recognition of the Fc. Our results indicate that afucosylation of half the heterodimer is sufficient to produce ADCC-enhancement similar to that observed for a fully afucosylated antibody with wild-type Fc. However, the most dramatic effect on ADCC activity is observed when two carbohydrate chains are present rather than one, regardless of afucosylation state.

Introduction

Bispecific antibody technology continues to be an area of great interest in the pursuit of next-generation monoclonal antibody (mAb) therapeutics for human disease. A bispecific antibody is generally thought of as a single molecule containing two distinct Fab variable domains having monovalent specificity for two distinct antigens. One way of achieving bispecificity is by utilizing knobs-into-holes technology whereby complementary mutations are made in the C_H3 domain of each heavy chain (HC).[3] These noncovalent interactions, along with disulfide bridges in the hinge region, drive assembly toward heterodimer formation.

Previously, knobs-into-holes technology has been applied to the production of human full-length bispecific antibodies with a single common light chain (LC).[3,4] The use of a common LC, although helpful in minimizing combinatorial heterogeneity, remains a limitation in the development of novel therapeutics. More recently, bispecific production using knobs-into-holes technology has been further developed to include two distinct LCs.[1] In the aforementioned case, *E. coli* was the host, which eliminated the possibility of oligosaccharide addition. Here, we describe our production strategy using mammalian cell expression to produce glycosylated antibodies. In addition, we take advantage of the asymmetric structure of glycosylated knobs-into-holes antibodies to investigate various aspects of glycosylation and effector function.

Oligosaccharide addition begins in the endoplasmic reticulum (ER) and ends when the antibody is secreted from the Golgi apparatus. The carbohydrate chain attached at the conserved asparagine 297 (N297) in the C_H2 domain of the crystallizable fragment (Fc) is comprised of a core complex of N-acetylglucosamine (GlcNac) and mannose, followed by variable additions of galactose, sialic acid, fucose and bisecting GlcNac residues. Binding of lymphocyte receptors (FcγRs) to the Fc of the antibody catalyzes phagocytic and cytolytic biological responses that are known to play a significant role in various diseases.[5] Glycosylation of the Fc on N297 is an essential component of complex formation with FcγRIIIa[6] and subsequent immune response.[7-9]

*Correspondence to: Justin M Scheer; Email: scheer.justin@gene.com
Submitted: 07/01/13; Revised: 08/27/13; Accepted: 08/28/13
http://dx.doi.org/10.4161/mabs.26307

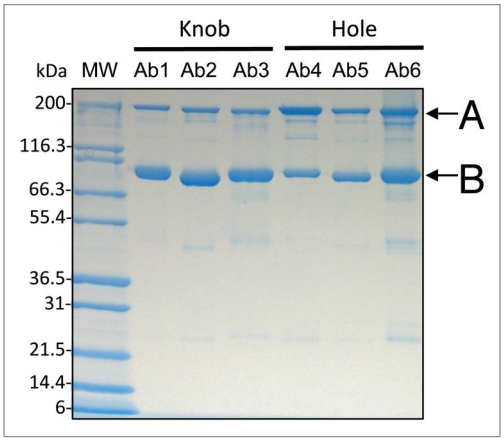

Figure 1. Production of knob and hole half-antibodies and homodimers in CHO. Six different antibodies with either knob or hole heavy chain mutations were produced. Protein-A affinity pools were analyzed by SDS-PAGE; the results indicate both the presence of half-antibody (**B**) and homodimer species (**A**). Covalent dimer content for hole production relative to knob was consistently higher.

Table 1. Heterodimeric pairs

Sample Name	Host Cell (Knob/Hole)	Structure
H1	*E.coli*/CHO	
H2	*E.coli*/Fut8KO	
H3	CHO/CHO	
H4	Fut8KO/CHO	
H5	CHO/Fut8KO	
H6	Fut8KO/Fut8KO	

In an endogenous setting, FcγR activities such as antibody-dependent cell-mediated cytotoxicity (ADCC) play a critical role in immune defense against infectious diseases. ADCC is initiated when the Fab portion of an antibody binds an antigen on a cell, targeting it for destruction. Fcγ receptors on the surface of an effector cell also bind to the antibody, but through the Fc portion, which triggers the release of cytokines and cytotoxic granules that infiltrate the cell and promote cell death. In particular, FcγRIIIa expressed on peripheral blood mononuclear cells (PBMC) or natural killer cells (NK) has been shown to play a pivotal role in ADCC activity.[10] Moreover, it has been demonstrated that antibodies with increased affinity for FcγRIIIa have improved cytolytic activity.[5,11] ADCC is also recognized for its involvement in the destruction of tumor cells.[12,13] This type of immune response is considered a specifically relevant mechanism of action for therapeutic antibodies.[14] Indeed, a polymorphism (Phe/Val 158) in FcγRIIIa resulting in higher affinity binding has been linked to clinical efficacy of anti-CD20 therapy in non-Hodgkin lymphoma patients.[15-17]

Although the Fc is a homodimer, FcγRIIIa binds in an asymmetric fashion[18] with 1:1 (Fc:FcγRIIIa) stoichiometry, making non-equivalent interactions with each polypeptide chain of the Fc. This complex appears to be mediated in part by a unique carbohydrate-carbohydrate interaction between the receptor and Fc.[19] Although oligosaccharide adducts on the Fc and FcγRIIIa have been shown to stabilize this interaction, challenges persist in controlling glycoform fidelity.[17] Many studies have demonstrated, however, that removal of the penultimate fucose ("afucosylation") from the Fc glycan results in a dramatic increase in FcγRIIIa affinity[19,20] and ADCC activity.[7,21,22] Indeed, expression cell lines where the fucosyltransferase has been knocked out (Fut8KO) have been described,[23] and several afucosylated antibody therapeutics are being developed.

Thus far, the effect of knobs-into-holes mutations in the C_H3 on clinically relevant effector function mechanisms has been minimally characterized.[3] Here, we use our bispecific assembly process based on separate expression of knob and hole H-L fragments to interrogate effector function mechanisms. The utility is demonstrated through production of an effector-function competent, mono-functional anti-CD20 antibody. Furthermore, we used our technology to specifically probe the effects of glycosylation asymmetry in ADCC, something that has yet to be done in a systematic way. Through production in various hosts, we demonstrate that fucose removal of only one chain of the heterodimer is sufficient to garner full enhancement of ADCC activity.

Results

Isolation and characterization of heterodimeric pairs. Mammalian derived transiently expressed half-antibodies eluted as a mixture of monomeric heavy-light half antibody (H-L) fragments and covalent homodimers (**Fig. 1**), with titers between 5 mg/L and 96 mg/L (**Table S1**). Each heterodimer was assembled by combining two H-L fragments from the following host systems: Chinese hamster ovary (CHO), Fut8KO and *E. coli*. A total of six heterodimers were assembled and characterized as described in Materials and Methods and shown in **Table 1**. Reduction and/or oxidation (redox) was performed at room temperature using an excess of L-reduced glutathione (GSH), enabling the breakdown of homodimers and formation of energetically favored heterodimers (**Fig. 2**). Upon completion of redox, between 75–85% of the mixture was assembled requiring one further polishing step to reach greater than 98% covalent antibody (**Fig. 3**). LC-ESI/TOF performed under non-reducing conditions confirmed two non-identical HCs for all six heterodimeric pairs and no detectable homodimer (**Fig. 4**). Both the theoretical and measured heterodimer masses were in agreement (within 5 Daltons) with outcarbohydrates, after deglycosylation (**Table S2**). Size exclusion chromatography-multi-angle laser light scattering (SEC-MALS) confirmed greater than 99% monomer (**Fig. 3C**).

Glycan structure. Glycan analysis of the oligosaccharides linked to the Fc revealed differences in glycan composition

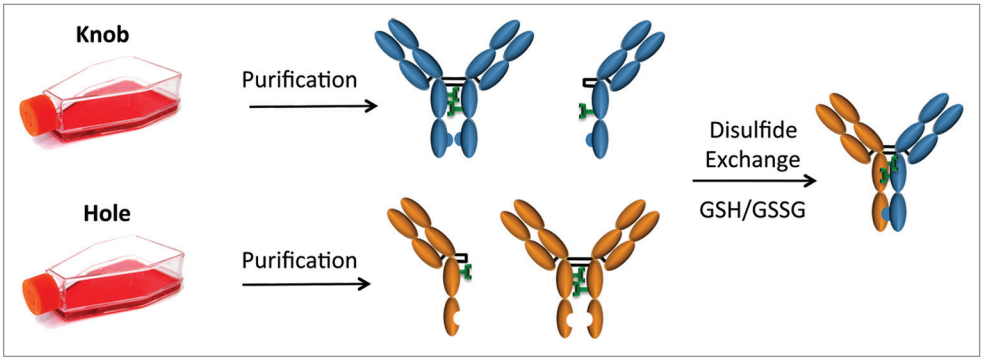

Figure 2. Bispecific assembly and disulfide formation after isolation from mammalian cell culture. Shown here is a schematic for the process of bispecific antibody production after mammalian cell expression with either knob or hole mutations. Variants are purified by Protein-A after individual expression, mixed and assembled into heterodimeric pairs using reduced glutathione disulfide exchange.

(**Fig. 5**; **Fig. S1**). CHO-derived hole H-L fragments contained approximately 1.2% afucosylation and 2.2% structures containing sialic acid while its knob counterpart contained about 4.4% afucosylated structures and greater than 20% sialation. These differences were clearly visible by mass spectrometry (MS) (**Fig. 6**). Furthermore, CHO-produced anti-CD20 without Fc mutations (WT) was 8% afucosylated, whereas 2.2% of the carbohydrates linked to the knobs-into-holes heterodimer (H3) lacked core fucose. Additionally, H3 contained about 10% sialic acid attached to one or the other galactose, whereas less than 1% sialation was detected on WT carbohydrate structures. As expected, the H-L fragments grown in Fut8KO cells contained similar biantennary structures, but lacked core fucose (**Fig. S1**). Similarly to H3, the Fut8KO version (H6) had higher levels of sialic acid (10.6%) compared with the WT grown in the same cell line (0.5%) (**Fig. 5**; **Fig. S1**).

Antigen binding activity. Binding of heterodimers to target cells was measured with a cell-based assay using WIL2-S cells, which express a high level of target antigen (CD20) on the cell surface.[24] Since there is no glycosylation site in the CDRs of these heterodimers, changes in the fucosylation level should not affect binding to cell surface target antigens. A summary of CD20 binding to heterodimeric pairs and asymmetric antibodies are presented in **Table 2**. As expected, there were no discernible differences in CD20 binding among heterodimers tested. CD20 binding was equivalent to the anti-CD20 antibody with wild-type Fc indicating no effect of the knobs-into-holes mutations on antigen affinity.

Fcγ receptor binding and ADCC activity. The Fcγ receptor binding activity of heterodimers was measured by ELISA-based methods using IIIa-F158 and IIIa-V158 of recombinant human Fcγ receptors.[24] ADCC activity was assessed using a human B lymphoma cell line, WIL2-S, as target cells and an engineered NK cells line as effector cells.[24] The heterodimer assembled from production in CHO cells (H3) showed reduced binding to FcγRIIIa and decreased potency relative to WT as shown in **Table 2**. Furthermore, ADCC activity of H3 with sialic acid removed (EC_{50} = 10.5 ng/mL) remained low relative to WT (EC_{50} = 1.43 ng/mL), but statistically indistinguishable from H3 with sialic acid present (EC_{50} = 8.3 ng/mL), suggesting that increased sialylation does not influence ADCC activity. In contrast, fucose exhibited a dramatic influence on heterodimer potency (**Table 2**; **Fig. 7**). Completely afucosylated heterodimer (H6) demonstrated ADCC activity equivalent to afucosylated WT (**Fig. 7**). Furthermore, heterodimers containing only one monomer grown in Fut8KO (H4 and H5) exhibited ADCC activities statistically comparable to completely afucosylated test antibodies (**Fig. 7**). These results were repeated twice with the NK cell line and were also observed with two different donor sources of PBMCs (**Fig. S2**). The relative mean potencies from all four assays are reported in **Table 2**, exhibiting a robust trend in agreement.

The relationship between glycosylation symmetry and activity was further probed by examining heterodimers with asymmetric glycosylation (**Table 1**). Though these hemi-aglycosylated heterodimers (H1 and H2) exhibited weak ADCC activities, they were not completely inactive (**Fig. 8**). Moreover, afucosylation levels of 1.1% for H1 and 27.3% for H2 remained consistent with the measurable difference in potency between them. These data suggest that fucose removal has notable consequences even at low levels of effector function activity.

Statistical analysis was performed to understand the trend in data. Both linear and nonlinear regression models were tried. Nonlinear regression provided the best fit for the data. To understand statistical significance of the trend, additional analysis was done using two-way ANOVA and the Tukey multiple comparisons test.

Discussion

Knobs-into-holes technology has become the foundation for a well-developed *E. coli* bispecific antibody production process, offering biochemical qualities comparable to conventional monoclonal antibodies and scalable manufacture compatible with large-scale production.[1] Moreover, validation of knobs-into-holes technology as a component of a therapeutic molecule has recently been established in Phase 2 clinical trials.[2] Here, we apply knobs-into-holes technology to mammalian-host production systems to produce glycosylated heterodimeric antibodies using an in vitro assembly method. Our approach is not dissimilar to processes described by Strop et al.[25] and Labrijn et al.,[26] where complementary mutations in the heavy chains allow favored recombination of heterodimeric pairs. However, unlike knobs-into-holes technology, these processes require additional mutations in the hinge core region to achieve efficient heterodimer formation. Despite these minor differences, these methods appear straightforward

and amenable to high-throughput production, thus demonstrating a selection of strategies for the production of bispecific antibodies.

Seventeen distinct H-L fragments were produced with knobs-into-holes mutations in various mammalian cell lines (**Table S1**). Transient expression patterns in CHO were similar to *E. coli* shake-flask titers and stable cell lines were comparable to *E. coli* fed-batch cultures (**Table S1**). It is interesting to note the abundance of homodimer in mammalian-host H-L fragment cultures (**Fig. 1**), whereas H-L fragments derived from *E. coli* are generally found to be monomeric.[1] Nonetheless, heterodimers derived from mammalian hosts retained conventional characteristics such as ease of assembly, purification and minimal aggregation (**Fig. 3**).

In addition, because antibodies produced from mammalians hosts are secreted with glycosylation, effector function mechanisms are enabled. Fc effector activity can be an asset in the development of biotherapeutics and the ability to manipulate it in the context of knobs-into-holes technology opens new possibilities for tailoring the activity of antibodies. Though the affect of such mutations on effector function has previously been examined,[3] the reported results were within the context of single cell production, with the use of a common LC. Here, we validate ADCC activity from heterodimers produced from separate H-L fragment expression and utilize this approach to manipulate glycan structure in an effort to understand the effects of symmetry on ADCC.

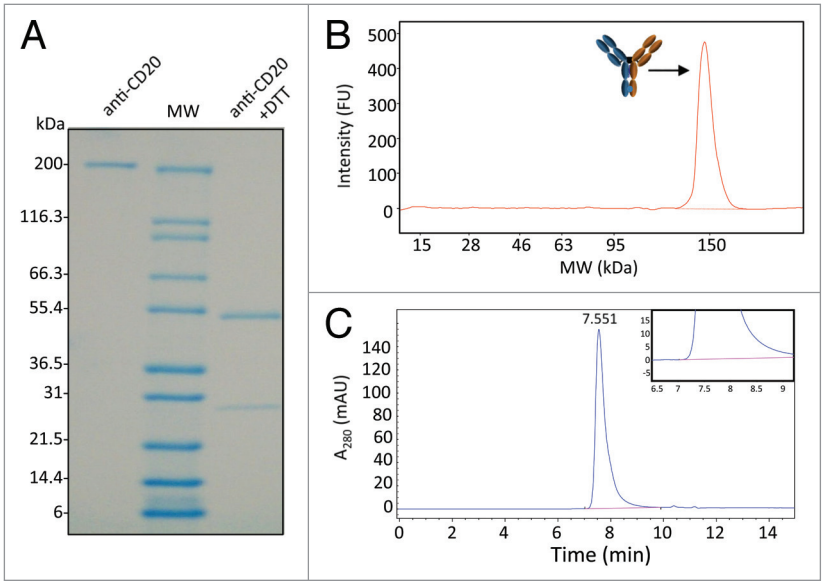

Figure 3. Characterization of CHO-derived heterodimer (H3) reveals high purity and minimal aggregation. (**A**) SDS-PAGE analysis of final product shows no visible impurities. The protein was analyzed both in the intact form and under reducing conditions (+DTT). Under reducing conditions, only one HC band is expected due to negligible differences in mass between the two chains. (**B**) Agilent Bioanalyzer electropherogram of the final product revealed > 99% 150 kDa. The absence of signal at 75 kDa demonstrates that no H-L fragments or non-covalent homodimer are present in the final product. (**C**) Chromatogram of size exclusion chromatography (SEC) of heterodimer (H3). The inset shows a zoomed-in view indicating no detectable aggregates or residual H-L fragments.

Initially, when ADCC activities of knobs-into-holes antibodies produced by in vitro assembly were compared with antibodies with WT Fc, the activity was substantially less. Analysis of N-linked oligosaccharide content of H-L fragments and heterodimer revealed significant glycovariation not typical for a regular antibody (**Fig. 5**). In antibody folding, H-L fragments spontaneously dimerize in the ER and Golgi before oligosaccharide addition begins. Since H-L fragment secretion is not a part of normal cell physiology, uncommon carbohydrate additions may be the result of increased accessibility of H-L fragments during post-translational processing. This may be especially true for knob H-L fragments, which exhibited high levels of sialic acid and fucose adducts (**Fig. 5**). We speculate that, due to the bulky nature of the knob mutation in the C_H3 domain, conventional homodimers are not readily formed (**Fig. 1**), possibly exposing the C_H2 domain in an unusual manner that is susceptible to additional carbohydrate residues. In the case of hole H-L fragments, homodimer was visibly more abundant (**Fig. 1**) and complex oligosaccharide addition less so (**Fig. 6**). This reinforces the idea that, in mammalian hosts, hole H-L fragments behave more like full antibodies. It is important to note that the atypical glycosylation processing seen for H-L fragments produced transiently may be overcome during stable cell line development. Because expression levels are generally significantly higher in stable cell lines, dimer formation may be more prevalent, thus eluding long chain additions during cellular processing.

To determine the influence of atypical glycosylation patterns on ADCC activity, sialic acid adducts on H3 were removed and heterodimer activity compared with WT. Sialic acid removal induced no change in potency, suggesting it has no influence on ADCC. However, it is known that ADCC activity of this anti-CD20 antibody is sensitive to fucose removal, resulting in significant increases in ADCC activity.[27] To determine whether fucose is the cause of H3's lowered activity, completely afucosylated knobs-into-holes heterodimer (H6), WT and afucosylated WT (AF WT) were compared. Without core fucose, the ADCC activity of H6 was completely restored, reaching AF WT levels (**Fig. 7**; **Fig. S2**). Clearly, the lower activity observed for H3 is a result of higher fucose levels associated with transient expression of H-L fragments in CHO cells. We maintain, as noted by Merchant et al.,[3] knobs-into-holes mutations in the context of this anti-CD20 antibody do not have a direct, negative effect on FcγR-binding and effector function. Thus with respect to this anti-CD20 antibody, the decreased FcγRIIIa-binding and ADCC activity of H3 are the result of altered glycan composition (**Fig. 5**), not the knobs-into-holes mutations.

Although afucosylation as a tool for boosting ADCC activity is known, the question of whether one or both Fc-fucose residues need to be absent for increased binding activity toward FcγRIII has been challenging to answer in a quantitative manner. Thus far, the only activity data that has been reported in the scientific

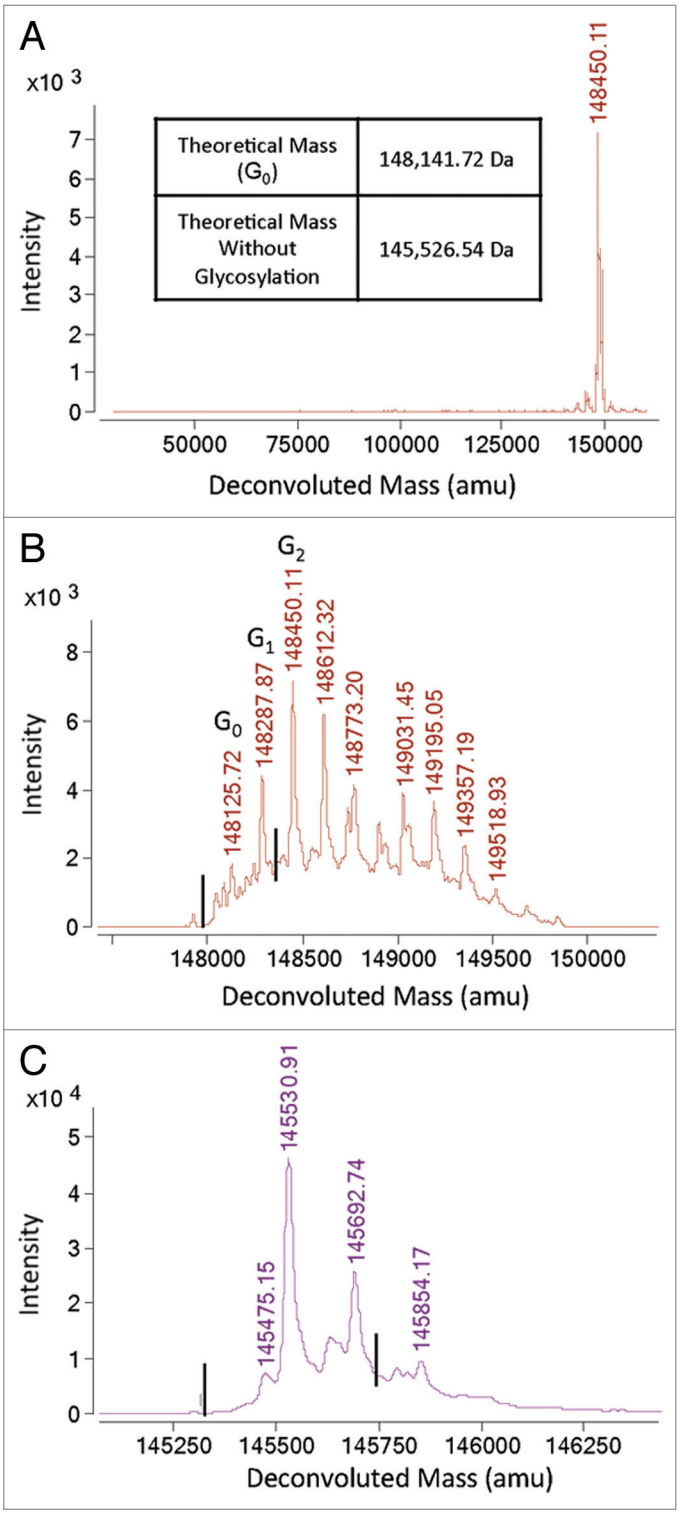

Figure 4. Mass spectrometry (MS) analysis of heterodimer (H6). (**A**) Bispecific antibody product shown in **Figure 3** was analyzed by LC-MS using and Agilent ESI-TOF as described in the Materials and Methods. Here we show the deconvoluted spectrum over a mass range of 20,000–160,000 amu, indicating the purity of the heterodimeric antibody. (**B**) A zoomed-in view of the deconvoluted mass spectrum shown in (a) indicates that there are no detectable homodimers. Masses of 148,346.98 Da for knob homodimer and 147,936.46 Da for hole homodimer were not detectable. The lines indicate the expected location of homodimer signals. (**C**) PNGase treatment was used to remove glycosylation heterogeneity to improve resolution and decrease complexity of the signal. Masses of 145,731.80 Da for knob homodimer and 145,321.28 Da for hole homodimer were not detectable. The lines indicate the expected location of homodimer signals.

literature examined antibody samples carrying mixtures of fucosylated or afucosylated glycans[24] and not hemi-afucosylated antibodies. With knobs-into-holes technology, each H-L fragment is produced separately, allowing greater independent control over glycan composition. This strategy has allowed a detailed examination of the effect of removal of one or both fucose residues on enhancement of ADCC activity.

The structure-activity relationship was examined by producing asymmetric heterodimers composed of H-L fragments with distinct glycoform (H1, H2, H4, and H5) and comparing ADCC activity and FcγRIIIa binding. As presented in **Figure** 7, the hemi-afucosylated heterodimers (H4 and H5) behave virtually identical to the fully afucosylated version. Statistically negligible differences in ADCC are observed between H4 (51.2% afucosylation), H5 (54.4% afucosylation) and H6 (100% afucosylation) despite prominent differences in fucose content (**Fig.** 7). Equivalently, approximately 50% afucosylation is enough to induce a high affinity interaction between asymmetric heterodimer and FcγRIIIa (**Table 2**). This relationship held true when the assay was repeated both with an engineered cell line and with different blood donors (**Table 2**; **Fig. S2**). These results are consistent with structural studies on complexes of afucosylated antibodies with glycosylated FcγRIIIa,[18,28] whereby the carbohydrate from the receptor interacts with only 1 of the 2 glycan chains of the Fc. Here, we used a defined hemi-afucosylated antibody to demonstrate that afucosylation on one glycan chain is sufficient to have the desired activity enhancement.

To probe the question of glycosylation symmetry further, heterodimers were assembled using one H-L fragment containing no glycosylation (derived from *E. coli*) and one H-L fragment derived from CHO or Fut8KO. A previous attempt using chromatographic techniques to enrich for homogenous hemi-glycosylated antibody reported a 3.5-fold decrease in ADCC compared with the fully-glycosylated antibody.[27] However, this study was hampered by incomplete resolution of the hemi- and fully-glycosylated forms of the antibody. In addition, the fucosylation status of the two forms was undetermined. In our study, where ADCC activities were measured from homogenous pools and fucose content was controlled, we observed diminished potencies for both hemi-glycosylated (H1) and hemi-glycosylated–hemi-afucosylated heterodimers (H2) relative to WT and fully-glycosylated heterodimer (H3) (**Fig. 3**). Furthermore, though afucosylation has a measurable effect on ADCC activity of H2, the impact is far greater when both heavy chains are glycosylated (**Fig. 8**). Glycosylation is thought to maintain the Fc in an "open" conformation competent for FcγR-binding.[29] Although glycosylation on one chain can render a partially open state, glycosylation of both chains may be necessary to complete the conformational transition.[30] Together these observations imply that though glycosylation of

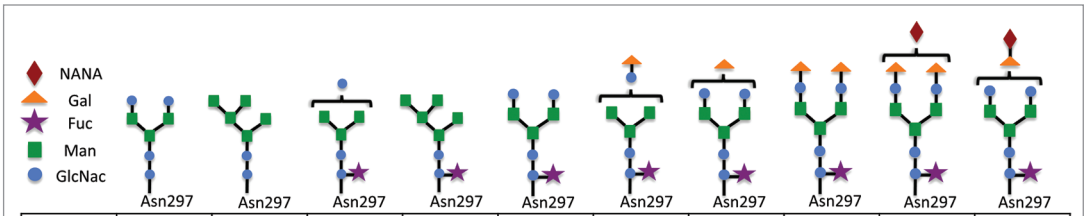

	G_0-F	ManX-F	G_0-1	Man5	G_0	G_1-1	G_1	G_2	G_2+NANA	G_1+NANA
WT	7.6	0.0	4.7	0.0	49.4	2.0	29.0	2.9	0.0	1
knob/hole (H3)	0.0	2.2	1.7	1.7	35.6	1.2	31.1	14.7	10.1	1.3
knob (H3)	0.0	4.4	1.3	0.0	25.3	1.6	24.5	20.6	17.1	4.3
hole (H3)	1.2	0.0	1.3	0.0	51.9	1.9	25.1	13.8	1.6	0.6

Figure 5. Quantitation of N-linked carbohydrate species. Relative quantitation of N-linked carbohydrate species using GlycoChip glycan analysis reveals fluctuations in glycan composition in pools where either knobs and/or holes mutations have been made. Most notably, an increase in core fucose and sialic acid content is observed in the knobs-into-holes antibody structures with respect to WT.

Table 2. Activities (EC_{50}) of each heterodimer were assessed by three different assays

Sample ID	Structure	% AF*	CD20 (μg/mL)	FcγRIIIa-V158 (μg/mL)	FcγRIIIa-F158 (μg/mL)	ADCC-NK (ng/mL)	ADCC-PBMC#1 (ng/mL)	ADCC-PBMC#2 (ng/mL)
WT	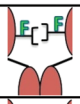	7.60	0.43	0.37	1.14	1.43	4.76	2.12
H1		1.10	ND	ND	ND	26.40	ND	ND
H2	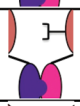	100.00	ND	ND	ND	14.90	ND	ND
H3		2.20	0.58	0.81	2.00	8.61	26.20	13.60
H4		51.20	0.72	0.06[a]	0.06[b]	0.34[c]	0.84[d]	0.37[e]
H5		54.40	0.52	0.07[a]	0.07[b]	0.28[c]	0.59[d]	0.24[e]
H6	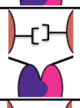	100.00	0.53	0.04[a]	0.04[b]	0.23[c]	0.43[d]	0.20[e]
AF WT	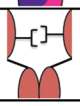	100.00	0.49	0.04[a]	0.04[b]	0.19[c]	0.36[d]	0.16[e]

*afucosylation; [a,b,c,d,e]These values are not statistically different from one another. Binding of heterodimers to CD20 antigen was measured using a cell-based electrochemiluminescent assay, heterodimer affinities toward FcγRIIIa were measured by ELISA and ADCC potencies via a cell-based killing assay. Within each column, EC_{50} values were assessed using two-way ANOVA and the Tukey multiple comparisons test to examine how the EC_{50}s were affected by core fucose levels within a receptor isotype or cell type. Superscript letters denote values that were found to be statistically indistinguishable from one another. Some assay values were not determined as denoted by "ND."

both monomers is critical, afucosylation of half is sufficient to profoundly influence ADCC.

Here, we described our efforts to produce effector function competent heterodimers with knobs and holes mutations in the Fc. Our results indicate that afucosylated heterodimers assembled using knobs-into-holes technology have comparable activity to controls, providing direct evidence for the viability of the technology for developing bispecific therapeutics retaining

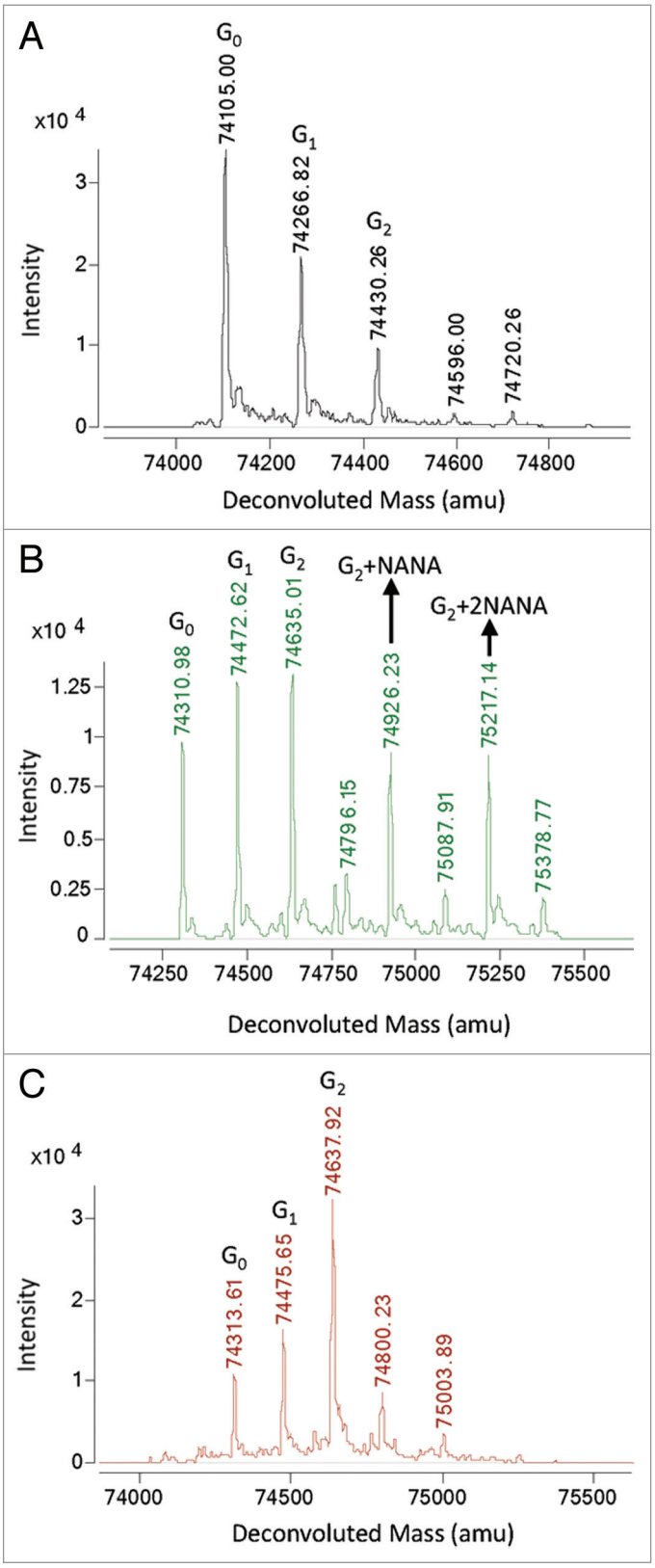

Figure 6. Deconvoluted mass spectrum of CHO-produced half-antibodies. (**A**) The deconvoluted mass spectrum of hole half-antibody shows a glycosylation pattern similar to a normal antibody. (**B**) The deconvoluted spectrum of knob half-antibody shows a more complicated glycosylation profile, dissimilar from hole shown in (a) and from a regular antibody. (**C**) The knob antibody was treated with neuraminidase to assess for the presence of sialic acid. The treated antibody shows a reduced complexity that is similar to the hole shown in (**A**).

ADCC. In addition, knobs-into-holes technology has given us the opportunity to gain refined insight into the structure-activity relationship between fucose and effector function. Our findings suggest that, although glycosylation of both chains appears to be necessary to stabilize Fc-receptor interactions, afucosylation of half of the dimer is sufficient for enhanced ADCC activity. These insights may allow application of the knobs-into-holes technology to the control of glycan composition for each monomer independently, offering advantages in the design and production of novel biopharmaceutical agents.

Materials and Methods

Expression. Anti-CD20 antibody (WT) was produced in CHO cells.[31] Heterodimers were made from separately expressed heavy-light chain half antibody (H-L) fragments in the following cell type: *Escherichia coli* (*E. coli*),[1] CHO and Fut8 Knock Out (Fut8KO).[23]

Isolation. Each H-L was captured on a 5 mL GE Healthcare MabSURE SELECT column. The column was then washed with 10 column volumes (CV) of an equilibration buffer consisting of 50 mM TRIS pH 8.0, 150 mM NaCl, 0.05% Triton X-100, 0.05% Triton X-114 and a wash buffer consisting of 25 mM sodium citrate, pH 6.0. Each H-L fragment was eluted with 0.15 M sodium acetate, pH 2.7.

Assembly, reduction, and oxidation. Knobs-into-holes technology[3] was used to produce heterodimers. Knob and hole H-L fragments and homodimers were independently titrated up to pH 5.0 using 1:10 1 M TRIS arginine pH 9.0 then combined together at a ratio of 1:1. The mixture was then titrated to pH 8.5 using 1:10 1 M TRIS-Arginine pH 9.0, and left at room temperature for three days following the addition of an excess of freshly prepared 0.5 M reduced L-Glutathione (Sigma Aldrich) at a molar ratio of 1:200.

Polishing. Following redox, the assembled heterodimers were loaded onto a 5 mL GE Healthcare SP HP column. The column was washed with 5 CVs of 25 mM sodium acetate pH 5.0 then eluted with 1 M NaCl over 30 CVs. Fractions (0.5 mL) were collected and peak fractions were separated by 4–20% Tris-Glycine SDS-PAGE to analyze purity and pooled accordingly.

Characterization. The molecular weight of each heterodimer was confirmed by liquid chromatography electrospray ionization with time-of-flight (LC-ESI/TOF) analysis using a PLRP-S column (4.6 × 50 mm). The mobile phases used were solvent A (0.05% trifluoroacetic acid (TFA) in water) and solvent B (80% acetonitrile, 20% water, 0.05% TFA); a gradient from 34% to 45% solvent B was applied to separate the polypeptides. The samples were analyzed directly, after deglycosylation with PNGase (Sigma Aldrich) and in certain cases after treatment with neuraminidase (Sigma Aldrich). Purity was analyzed by 4–20% Tris-Glycine SDS PAGE gel and Agilent Bioanalyzer Series

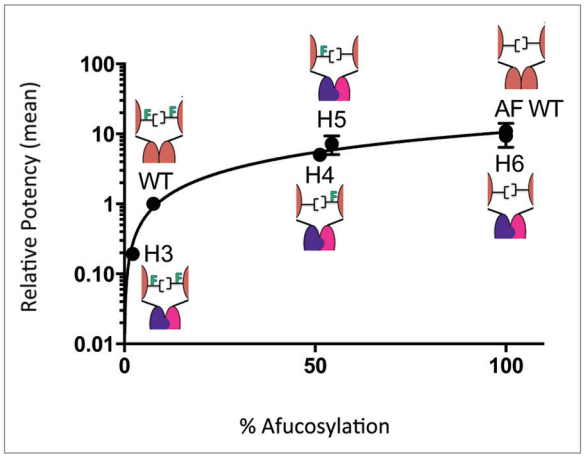

Figure 7. ADCC potencies have a nonlinear correlation to the percentage of afucosylation. Relative mean ADCC potencies were calculated from four independent assays using an engineered NK cell line and PBMCs from two different donors. Values were plotted against their corresponding fucose levels and normalized to WT. The data fits well into a nonlinear regression model demonstrating that the absence of only one core fucose is required to achieve high potencies similar to complete afucosylation. All replicates are in close agreement with one another.

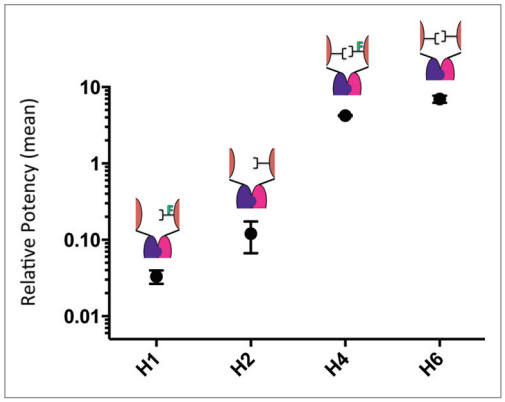

Figure 8. Glycosylation symmetry has a greater influence on ADCC than does afucosylation symmetry. In this figure we compare four distinct variants of carbohydrate composition, all of which are achieved by using heterodimer assembly technology described herein. The ADCC activities have been measured using an engineered NK cell line (assayed twice on two different days) and have been reported as relative values; normalized to WT. Shown here is the ability to tune ADCC activity with asymmetric carbohydrate composition. The graph suggests that though afucosylation of a hemi-glycosylated antibody influences ADCC activity, symmetry of glycosylation garners a more significant impact.

230 II. Aggregate levels were determined by SEC-MALS using a Sepax ZENIX SEC-300 column (7.8 × 300 mm) run under isocratic conditions using phosphate buffered saline (PBS) pH 7.2, 150 mM NaCl.

Glycan analysis. Two micrograms (μg) of each sample were loaded onto the mAB-Glyco Chip (Agilent Technologies). On-chip N-linked deglycosylation of each samples and chromatographic separation of glycans from proteins was performed, followed by Q-TOF detection of the cleaved glycans.[32,33]

CD20 binding assay. Binding of heterodimer to CD20 antigen was measured using a cell-based electrochemiluminescent assay as described by Lu et al.[34] WIL2-S cells, a human B lymphoma cell line expressing a high level of CD20, were washed with PBS and seeded at 25,000 cells per well in 25 μL PBS on 96-well MULTI-ARRAY High Bind plates (MSD). WIL2 cells were incubated for one hour at room temperature (RT) to allow cell attachment to the carbon surface. The plates were then blocked with 15% FBS in PBS for 30 min at RT with mild agitation and incubated with serial dilutions of heterodimers in assay buffer (PBS containing 10% FBS). After 1 h incubation at RT with mild agitation, the plates were washed and bound heterodimers were detected by adding ruthenium-labeled $F(ab')_2$ goat anti-human IgG Fc in assay buffer in the presence of Tris-based Read Buffer T (MSD). Upon electrochemical stimulation, luminescent signals were quantified with a Sector Imager 6000 reader (MSD). Dose-response binding curves were generated by plotting the mean luminescent signals from the duplicates of sample dilutions against the sample concentrations and fitting the data points to a four-parameter model using SoftMax Pro (Molecular Devices).

Fcγ receptor binding by ELISA. The binding activities of test antibodies toward various human Fcγ receptors were assessed by ELISA-based ligand binding assays.[10] The human FcγR were expressed as fusion proteins containing the receptor extracellular domain linked to a Gly/6x His/glutathione S-transferase (GST) polypeptide tag at the C-terminus. For the low-affinity receptor (FcγRIIIa), heterodimers were tested as multimers by cross-linking with $F(ab')_2$ fragments of goat anti-human kappa chain antibodies (MP Biomedicals) at a molar ratio of 1:3. Sample and reagent dilutions were prepared in an assay buffer containing PBS, 0.5% BSA and 0.05% Tween-20. Plates were washed with PBS containing 0.05% Tween-20 using an ELx405™ plate washer (Biotek Instruments) after each incubation step.

Plates were coated with an anti-GST antibody (Genentech) in a 0.05 M sodium carbonate buffer (pH 9.6) overnight at 4 °C. After blocking with the capture antibody, the plates were incubated with receptor-GST fusion for 1 h at RT. Serially diluted heterodimers were added as multimeric complexes and the plates were incubated for 2 h at RT. Heterodimers bound to the receptor were detected by adding HRP conjugated $F(ab')_2$ fragment of goat anti-human $F(ab')_2$ (Jackson ImmunoResearch Laboratories) followed by substrate TMB (Kirkegaard and Perry Laboratories). The plates were incubated for 20 min at RT to allow for color development. The reaction was terminated with 1 M H_3PO_4 and absorbance determined at 450 nm. Dose-response binding curves were generated by plotting the mean absorbance values from duplicates of sample dilutions against the sample concentrations and fitting the data points to a four-parameter model using SoftMax Pro (Molecular Devices) to obtain the EC_{50} values. For comparison, relative activity was calculated for each sample by inversely normalizing its EC_{50} value with that of a reference molecule using the following formula:

Relative activity = EC_{50} reference/EC_{50} sample

Antibody-dependent cell-mediated cytotoxicity assay. ADCC assays were performed using PBMC from healthy

donors as effector cells and WIL2-S, a human B-lymphoma cell line, as target cells. PBMC were isolated from fresh blood of two healthy human donors by density gradient centrifugation. Target cells (4×10^4) prepared in assay medium (RPMI 1640 with 1% BSA and 100 units/mL penicillin and streptomycin) were added to each well in round-bottom, 96-well tissue culture plates. Serial dilutions of antibodies (10,000 to 0.0038 ng/mL following 4-fold dilutions in series) were added to the plates containing the target cells (50 μL/well) and incubated for 30 min at 37 °C with 5% CO_2 to allow opsonization. After incubation, PBMC (1.0×10^6) were added to each well, in assay medium, for a 25:1 effector:target cell ratio and the plates were incubated further for 4 h. The plates were then centrifuged and the supernatants were assayed for lactate dehydrogenase activity using a Cytotoxicity Detection Kit (Roche Diagnostics Corporation). Cell lysis was quantified by measuring absorbance at 490 nm using a microplate reader SpectraMax® 190 (Molecular Devices). Absorbance of wells containing only the target cells served as the control for background (low control), whereas wells containing target cells lysed with Triton-X100 provided the maximum available signal (high control). Antibody independent cell-mediated cytotoxicity (AICC) was measured in wells containing target and effector cells without the antibody.

The extent of specific ADCC was calculated as follows:

% ADCC = [$A_{490\ nm}$ (sample - $A_{490\ nm}$ (AICC)]/[$A_{490\ nm}$ (high control) - $A_{490\ nm}$ (low control)]

Dose-response curves were generated by plotting the mean % ADCC values from duplicates of the antibody sample dilutions against the antibody concentrations. The EC_{50} values were calculated by fitting the data points to a four-parameter equation using SoftMax Pro. For comparison, relative activity was calculated for each sample by inversely normalizing its EC_{50} value with that of a reference molecule using the following formula:

Relative activity = EC_{50} reference/EC_{50} sample

In all experiments, an engineered NK cell line expressing stably transfected human FcγRIIIa-F158 was also used as effector cells,[35] but the effector:target cell ratio was changed to 5:1 and the incubation time was reduced to 3 h. The rest of the procedures were the same as described above.

In some cases, specific toxicity (ST) was determined using an engineered NK cell line derived from NK92 (Roche Glycart AG) as effector cells and DELFIA BATDA (Perkin Elmer) labeled WIL2-S cells as target cells. Cell lysis was measured using time-resolved fluorescence in relative fluorescence units (RFU) by excitation at 345 nm and quantifying emission at 615 nm using a microplate reader SpectraMax® 190 (Molecular Devices). Absorbance of wells containing only labeled target cells served as the control for background (background), whereas wells containing labeled target cells with DELFIA BATDA lysis buffer provided the maximum available signal (maximum release). Spontaneous release (SR) was measured from wells containing only target cells, whereas SR + NK was measured from wells containing both target and effector cells without antibody.

The percent specific toxicity (% ST) was determined according to the formula below:

% ST = [(specific release - background) - (spontaneous release - background)] ÷ [(maximum release - background) -(spontaneous release - background)] × 100

The dose response curves were generated by plotting the mean % ST from triplicates against the concentration of antibody sample in ng/mL using a 4-parameter fit. Data analysis was performed using parallel line analysis curve fitting software (PLA) from SOFTmaxPRO™, generating separate lines for the reference material and test material to estimate potency of the test material relative to the reference material.

Disclosure of Potential Conflicts of Interest

No potential conflicts of interest were disclosed.

Supplemental Materials

Supplemental materials may be found here:
www.landesbioscience.com/journals/mabs/article/26307

Acknowledgments

The authors would like to thank Athena Wong for providing the cell cultures, Jean-Michel Vernes and Gloria Meng for assay support, Lisa Berstein for support with data analysis, and Diego Ellerman for helpful feedback.

References

1. Spiess C, Merchant M, Huang A, Zheng Z, Yang NY, Peng J, Ellerman D, Shatz W, Reilly D, Yansura DG, et al. Bispecific antibodies with natural architecture produced by co-culture of bacteria expressing two distinct half-antibodies. Nat Biotechnol 2013; 31:753-8; PMID:23831709; http://dx.doi.org/10.1038/nbt.2621
2. Spigel DRET, Ramlau R, Daniel DB. Final efficacy results from OAM4558g, a randomized phase II study evaluating MetMab or placebo in combination with erlotinib in advanced NSCLC. J Clin Oncol 2011; 29:suppl abstr 7505.
3. Merchant AM, Zhu Z, Yuan JQ, Goddard A, Adams CW, Presta LG, Carter P. An efficient route to human bispecific IgG. Nat Biotechnol 1998; 16:677-81; PMID:9661204; http://dx.doi.org/10.1038/nbt0798-677
4. Jackman J, Chen Y, Huang A, Moffat B, Scheer JM, Leong SR, Lee WP, Zhang J, Sharma N, Lu Y, et al. Development of a two-part strategy to identify a therapeutic human bispecific antibody that inhibits IgE receptor signaling. J Biol Chem 2010; 285:20850-9; PMID:20444694; http://dx.doi.org/10.1074/jbc.M110.113910
5. Deo YM, Graziano RF, Repp R, van de Winkel JG. Clinical significance of IgG Fc receptors and Fc gamma R-directed immunotherapies. Immunol Today 1997; 18:127-35; PMID:9078685; http://dx.doi.org/10.1016/S0167-5699(97)01007-4
6. Radaev S, Motyka S, Fridman WH, Sautes-Fridman C, Sun PD. The structure of a human type III Fcgamma receptor in complex with Fc. J Biol Chem 2001; 276:16469-77; PMID:11297532; http://dx.doi.org/10.1074/jbc.M100350200
7. Wright A, Morrison SL. Effect of glycosylation on antibody function: implications for genetic engineering. Trends Biotechnol 1997; 15:26-32; PMID:9032990; http://dx.doi.org/10.1016/S0167-7799(96)10062-7
8. Rudd PM, Elliott T, Cresswell P, Wilson IA, Dwek RA. Glycosylation and the immune system. Science 2001; 291:2370-6; PMID:11269318; http://dx.doi.org/10.1126/science.291.5512.2370
9. Jefferis R, Lund J, Pound JD. IgG-Fc-mediated effector functions: molecular definition of interaction sites for effector ligands and the role of glycosylation. Immunol Rev 1998; 163:59-76; PMID:9700502; http://dx.doi.org/10.1111/j.1600-065X.1998.tb01188.x
10. Shields RL, Namenuk AK, Hong K, Meng YG, Rae J, Briggs J, Xie D, Lai J, Stadlen A, Li B, et al. High resolution mapping of the binding site on human IgG1 for Fc gamma RI, Fc gamma RII, Fc gamma RIII, and FcRn and design of IgG1 variants with improved binding to the Fc gamma R. J Biol Chem 2001; 276:6591-604; PMID:11096108; http://dx.doi.org/10.1074/jbc.M009483200

11. Ferrara C, Stuart F, Sondermann P, Brünker P, Umaña P. The carbohydrate at FcgammaRIIIa Asn-162. An element required for high affinity binding to non-fucosylated IgG glycoforms. J Biol Chem 2006; 281:5032-6; PMID:16330541; http://dx.doi.org/10.1074/jbc.M510171200
12. Hooijberg E, van den Berk PC, Sein JJ, Wijdenes J, Hart AA, de Boer RW, Melief CJ, Hekman A. Enhanced antitumor effects of CD20 over CD19 monoclonal antibodies in a nude mouse xenograft model. Cancer Res 1995; 55:840-6; PMID:7531616
13. Clynes RA, Towers TL, Presta LG, Ravetch JV. Inhibitory Fc receptors modulate in vivo cytotoxicity against tumor targets. Nat Med 2000; 6:443-6; PMID:10742152; http://dx.doi.org/10.1038/74704
14. Umaña P, Jean-Mairet J, Moudry R, Amstutz H, Bailey JE. Engineered glycoforms of an antineuroblastoma IgG1 with optimized antibody-dependent cellular cytotoxic activity. Nat Biotechnol 1999; 17:176-80; PMID:10052355; http://dx.doi.org/10.1038/6179
15. Grillo-López AJ, Hedrick E, Rashford M, Benyunes M. Rituximab: ongoing and future clinical development. Semin Oncol 2002; 29(Suppl 2):105-12; PMID:11842397; http://dx.doi.org/10.1053/sonc.2002.30145
16. Cartron G, Dacheux L, Salles G, Solal-Celigny P, Bardos P, Colombat P, Watier H. Therapeutic activity of humanized anti-CD20 monoclonal antibody and polymorphism in IgG Fc receptor FcgammaRIIIa gene. Blood 2002; 99:754-8; PMID:11806974; http://dx.doi.org/10.1182/blood.V99.3.754
17. Jefferis R. Glycosylation as a strategy to improve antibody-based therapeutics. Nat Rev Drug Discov 2009; 8:226-34; PMID:19247305; http://dx.doi.org/10.1038/nrd2804
18. Sondermann P, Huber R, Oosthuizen V, Jacob U. The 3.2-A crystal structure of the human IgG1 Fc fragment-Fc gammaRIII complex. Nature 2000; 406:267-73; PMID:10917521; http://dx.doi.org/10.1038/35018508
19. Ferrara C, Grau S, Jäger C, Sondermann P, Brünker P, Waldhauer I, Hennig M, Ruf A, Rufer AC, Stihle M, et al. Unique carbohydrate-carbohydrate interactions are required for high affinity binding between FcgammaRIII and antibodies lacking core fucose. Proc Natl Acad Sci U S A 2011; 108:12669-74; PMID:21768335; http://dx.doi.org/10.1073/pnas.1108455108
20. Okazaki A, Shoji-Hosaka E, Nakamura K, Wakitani M, Uchida K, Kakita S, Tsumoto K, Kumagai I, Shitara K. Fucose depletion from human IgG1 oligosaccharide enhances binding enthalpy and association rate between IgG1 and FcgammaRIIIa. J Mol Biol 2004; 336:1239-49; PMID:15037082; http://dx.doi.org/10.1016/j.jmb.2004.01.007
21. Shinkawa T, Nakamura K, Yamane N, Shoji-Hosaka E, Kanda Y, Sakurada M, Uchida K, Anazawa H, Satoh M, Yamasaki M, et al. The absence of fucose but not the presence of galactose or bisecting N-acetylglucosamine of human IgG1 complex-type oligosaccharides shows the critical role of enhancing antibody-dependent cellular cytotoxicity. J Biol Chem 2003; 278:3466-73; PMID:12427744; http://dx.doi.org/10.1074/jbc.M210665200
22. Shields RL, Lai J, Keck R, O'Connell LY, Hong K, Meng YG, Weikert SH, Presta LG. Lack of fucose on human IgG1 N-linked oligosaccharide improves binding to human Fcgamma RIII and antibody-dependent cellular toxicity. J Biol Chem 2002; 277:26733-40; PMID:11986321; http://dx.doi.org/10.1074/jbc.M202069200
23. Yamane-Ohnuki N, Kinoshita S, Inoue-Urakubo M, Kusunoki M, Iida S, Nakano R, Wakitani M, Niwa R, Sakurada M, Uchida K, et al. Establishment of FUT8 knockout Chinese hamster ovary cells: an ideal host cell line for producing completely defucosylated antibodies with enhanced antibody-dependent cellular cytotoxicity. Biotechnol Bioeng 2004; 87:614-22; PMID:15352059; http://dx.doi.org/10.1002/bit.20151
24. Chung S, Quarmby V, Gao X, Ying Y, Lin L, Reed C, Fong C, Lau W, Qiu ZJ, Shen A, et al. Quantitative evaluation of fucose reducing effects in a humanized antibody on Fcγ receptor binding and antibody-dependent cell-mediated cytotoxicity activities. MAbs 2012; 4:326-40; PMID:22531441; http://dx.doi.org/10.4161/mabs.19941
25. Strop P, Ho WH, Boustany LM, Abdiche YN, Lindquist KC, Farias SE, Rickert M, Appah CT, Pascua E, Radcliffe T, et al. Generating bispecific human IgG1 and IgG2 antibodies from any antibody pair. J Mol Biol 2012; 420:204-19; PMID:22543237; http://dx.doi.org/10.1016/j.jmb.2012.04.020
26. Labrijn AF, Meesters JI, de Goeij BE, van den Bremer ET, Neijssen J, van Kampen MD, Strumane K, Verploegen S, Kundu A, Gramer MJ, et al. Efficient generation of stable bispecific IgG1 by controlled Fab-arm exchange. Proc Natl Acad Sci U S A 2013; 110:5145-50; PMID:23479652; http://dx.doi.org/10.1073/pnas.1220145110
27. Ha S, Ou Y, Vlasak J, Li Y, Wang S, Vo K, Du Y, Mach A, Fang Y, Zhang N. Isolation and characterization of IgG1 with asymmetrical Fc glycosylation. Glycobiology 2011; 21:1087-96; PMID:21470983; http://dx.doi.org/10.1093/glycob/cwr047
28. Mizushima T, Yagi H, Takemoto E, Shibata-Koyama M, Isoda Y, Iida S, Masuda K, Satoh M, Kato K. Structural basis for improved efficacy of therapeutic antibodies on defucosylation of their Fc glycans. Genes Cells 2011; 16:1071-80; PMID:22023369; http://dx.doi.org/10.1111/j.1365-2443.2011.01552.x
29. Borrok MJ, Jung ST, Kang TH, Monzingo AF, Georgiou G. Revisiting the role of glycosylation in the structure of human IgG Fc. ACS Chem Biol 2012; 7:1596-602; PMID:22747430; http://dx.doi.org/10.1021/cb300130k
30. Krapp S, Mimura Y, Jefferis R, Huber R, Sondermann P. Structural analysis of human IgG-Fc glycoforms reveals a correlation between glycosylation and structural integrity. J Mol Biol 2003; 325:979-89; PMID:12527303; http://dx.doi.org/10.1016/S0022-2836(02)01250-0
31. Keen MJ, Rapson NT. Development of a serum-free culture medium for the large scale production of recombinant protein from a Chinese hamster ovary cell line. Cytotechnology 1995; 17:153-63; PMID:22358555; http://dx.doi.org/10.1007/BF00749653
32. Bynum MA, Yin H, Felts K, Lee YM, Monell CR, Killeen K. Characterization of IgG N-glycans employing a microfluidic chip that integrates glycan cleavage, sample purification, LC separation, and MS detection. Anal Chem 2009; 81:8818-25; PMID:19807107; http://dx.doi.org/10.1021/ac901326u
33. Trojer L GK, van de Goor T, Buckenmaier S. The mAb-Glyco Chip Kit - a Workflow Solution for Rapid and Fully Automated Characterization of N-linked Glycans from Monoclonal Antibodies. Chromatography Today 2011; August/September:16-21.
34. Lu Y, Wong WL, Meng YG. A high throughput electrochemiluminescent cell-binding assay for therapeutic anti-CD20 antibody selection. J Immunol Methods 2006; 314:74-9; PMID:16814318; http://dx.doi.org/10.1016/j.jim.2006.05.011
35. Schnueriger A, Grau R, Sondermann P, Schreitmueller T, Marti S, Zocher M. Development of a quantitative, cell-line based assay to measure ADCC activity mediated by therapeutic antibodies. Mol Immunol 2011; 48:1512-7; PMID:21570725; http://dx.doi.org/10.1016/j.molimm.2011.04.010